Radical Pathways for the Prebiotic Formation of Pyrimidine Bases from Formamide

ARTICLE *in* THE JOURNAL OF PHYSICAL CHEMISTRY A · JULY 2015

Impact Factor: 2.69 · DOI: 10.1021/acs.jpca.5b03625 · Source: PubMed

4 AUTHORS:

Huyen Thi Nguyen

12 PUBLICATIONS **55** CITATIONS

SEE PROFILE

Yassin A. Jeilani

Spelman College

16 PUBLICATIONS **45** CITATIONS

SEE PROFILE

Hung Minh

Quy Nhon University

3 PUBLICATIONS **1** CITATION

SEE PROFILE

Minh Tho Nguyen

University of Leuven

748 PUBLICATIONS **10,363** CITATIONS

SEE PROFILE

THE JOURNAL OF PHYSICAL CHEMISTRY A

Article

pubs.acs.org/JPCA

Radical Pathways for the Prebiotic Formation of Pyrimidine Bases from Formamide

Huyen Thi Nguyen,[†] Yassin A. Jeilani,[*,‡] Huynh Minh Hung,[†] and Minh Tho Nguyen[*,†]

[†]Department of Chemistry, KU Leuven, B-3001 Leuven, Belgium

[‡]Department Chemistry and Biochemistry, Spelman College, Atlanta, Georgia 30314, United States

Supporting Information

ABSTRACT: The prebiotic formation of nucleobases, the building blocks of RNA/DNA, is of current interest. Highly reactive radical species present in the atmosphere under irradiation have been suggested to be involved in the prebiotic synthesis of nucleobases from formamide (FM). We studied several free radical reaction pathways for the synthesis of pyrimidine bases (cytosine, uracil, and thymine) from FM under cold conditions. These pathways are theoretically determined using density functional theory (DFT) computations to examine their kinetic and thermodynamic feasibilities. These free radical reaction pathways share some common reaction types such as H-rearrangement, $^{\bullet}H/^{\bullet}OH/^{\bullet}NH_2$ radical loss, and intramolecular radical cyclization. The rate-determining steps in these pathways are characterized with low energy barriers. The energy barriers of the ring formation steps are in the range of 3−7 kcal/mol. Although DFT methods are known to significantly underestimate the barriers for addition of $^{\bullet}H$ radical to neutral species, many of these reactions are highly exergonic with energy release of −15 to −52 kcal/mol and are thus favorable. Among the suggested pathways for formation of cytosine (main route, routes **7a** and **1a**), uracil (main route, routes **7b** and **1b**), and thymine (main route and route **26a**), the main routes are in general thermodynamically more exergonic and more kinetically favored than other alternative routes with lower overall energy barriers. The reaction energies released following formation of cytosine, uracil, and thymine from FM via the main radical routes amount to −59, −81, and −104 kcal/mol, respectively. Increasing temperature induces unfavorable changes in both kinetic and thermodynamic aspects of the suggested routes. However, the main routes are still more favored than the alternative pathways at the temperature up to the boiling point of FM.

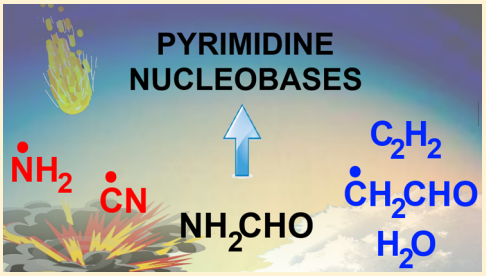

1. INTRODUCTION

The question of how nucleobases, the building blocks of RNA/DNA, were formed from the simple molecules that were present in the primordial Earth or in the extraterrestrial environment has attracted much interest.[1−8] Several prebiotic synthetic routes have been identified, for example, the formation of purines from HCN,[1] pyrimidines from HCCC/HCCCN[2] and β-alanine,[3] and both purines and pyrimidines from formamide (NH_2CHO, FM).[4−7] FM is an excellent prebiotic precursor that forms a wide range of biologically relevant compounds including nucleobases, amino acids, carboxylic acids, and other important intermediates in the prebiotic synthesis.[7,9−23] Various substances have been used to catalyze these reactions including calcium carbonate,[10,12] phosphates,[10,13] borate minerals,[14] zeolite, alumina and silica,[12] clays,[7,12,15] titanium dioxide,[7,11,16] iron sulfur and iron−copper sulfur,[17] iron oxide and iron oxide hydroxides,[18] zirconium minerals,[19] metal octacyanomolybdates,[20] cosmic dust analogues,[23] and meteorites.[7,21,22]

The addition of a catalyst is necessary for the synthesis of nucleobases when heating neat FM in the temperature range of 130−200 °C without irradiation because otherwise only purine is formed.[9,10] Irradiation with soft UV light (320 nm) during the heating process was proven to facilitate the production of other nucleobases even without adding catalyst.[7] Nucleobases can also be formed from FM under high-energy meteoritic impact conditions. Irradiation of ice or liquid FM with high-power laser beam yielded purine, glycine, and all five primary nucleobases.[7] In the latter experiment, the extremely high temperature of 4500 K in the laser spark creates hot dense plasma containing highly reactive radicals such as $^{\bullet}NH_2$, $^{\bullet}NH$, and $^{\bullet}CN$, which suggested an involvement of free radicals in the transformations.

Free radical participation in prebiotic formation of both purines and pyrimidines from FM was investigated.[5−8] Previous studies suggested that the radicals in the impact plasma,[7,8] which were present in the early Earth or in the extraterrestrial environment such as Titan,[5,6] played an important role in the formation of nucleobases. The free radical pathway is usually characterized by low energy barriers for connected steps and also by favorable thermodynamics. Furthermore, free radical mechanism also facilitates the highly diverse chemical transformation network from FM giving rise to formation of various nucleobases from a single prebiotic route. This is a remarkable

Received: April 15, 2015
Revised: July 21, 2015

DOI: 10.1021/acs.jpca.5b03625
J. Phys. Chem. A XXXX, XXX, XXX−XXX

Scheme 1. Possible Reaction Pathways Leading to Nucleobases from Formamide (FM)

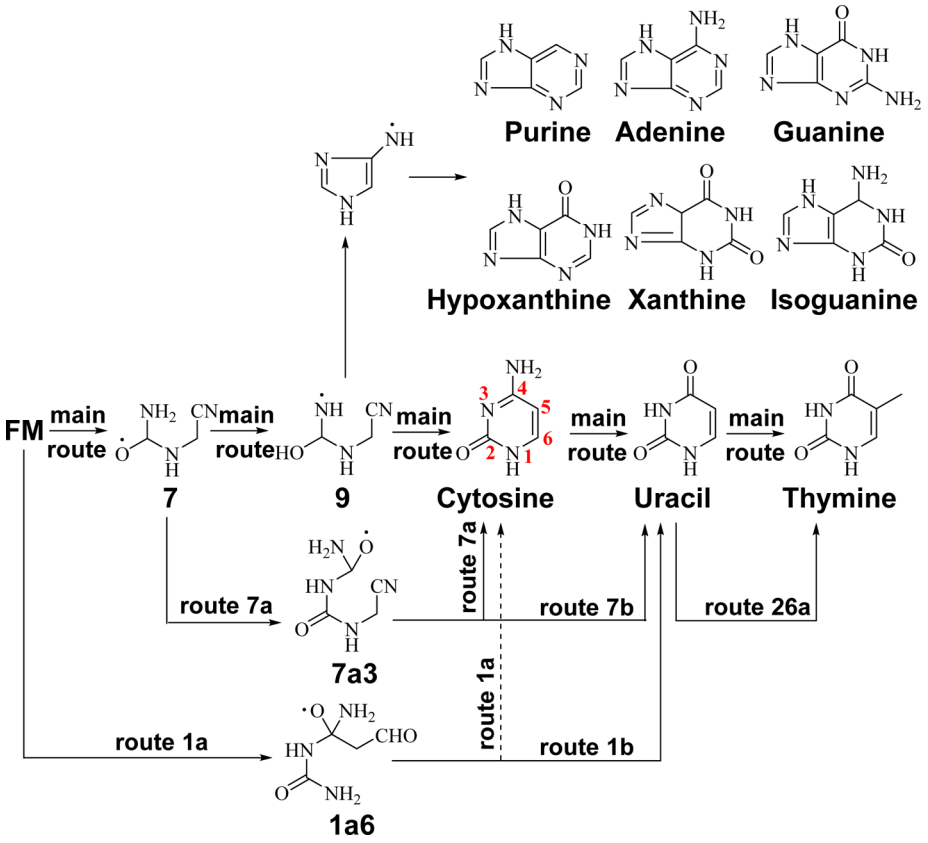

fact in many experiments where a mixture of different nucleobases was formed from FM under one single experimental condition. Cytosine, uracil, and thymine were all present in the product mixture with high yields when liquid FM was exposed to high-energy laser in the presence of clay.[7] Cytosine, 5-hydroxymethyluracil, thymine, and a trace of uracil were also simultaneously observed when neat FM was heated to 160 °C under sunlight irradiation with a small amount of TiO_2 powder as photocatalyst.[16] The type of pyrimidines and their yields significantly varied with the reaction conditions and the nature of catalysts. Under high-energy impact conditions, no catalyst was needed for formation of uracil and thymine from FM,[7] whereas the presence of montmorillonites was required for production of cytosine and uracil upon heating FM at 160 °C.[15] Despite numerous experimental reports, comprehensive reaction mechanisms of FM leading to pyrimidine bases, especially uracil and thymine, are still not available.

A detailed step-by-step free radical mechanism leading to purine, adenine, guanine, isoguanine, xanthine, and hypoxanthine was suggested and theoretically studied using density functional theory (DFT) methods.[5,6] Because the one-pot synthesis from FM can give both purines and pyrimidines,[7,12−22] it is reasonable to expect that a free radical route also leads to pyrimidines. In this context, we set out to perform quantum chemical computations to investigate the generation of nucleobases such as cytosine, uracil, and thymine from FM, and the small species, which were present in the prebiotic atmospheres (in particular of Titan) such as HCN, $^{\bullet}CN$, and $^{\bullet}NH_2$.

Alternative mechanisms leading to cytosine, uracil, and barbituric acid from FM and acetylene (C_2H_2) were also examined. The fact that sparking the gas mixture of CH_4 and N_2, the main gases in the atmosphere of Titan, gives acetylene as main product[24] has drawn attention to the prebiotic role of acetylene. Cold condition was considered as favorable prebiotic medium due to the stabilization effect of the ice matrix on the newly formed nucleobases.[25,26] Scheme 1 points out different routes that are appropriate for the cold condition of Titan atmosphere. This shows the main routes that are defined as FM → **7** → **9** → cytosine, uracil, thymine, and some alternative routes including the routes **7a**, **7b**, and **26a**, for the reactions from FM and HCN, and the routes **1a** and **1b** for the reactions from FM and acetylene. The precursor leading to the purine bases[5,6] is also specified in Scheme 1.

Note that these suggested routes are only a small part of a far more complicated network of possible reaction pathways leading to pyrimidines, and side radical reactions yielding other byproducts could take place from the reactant mixture. A comprehensive study of all the possible reactions in both thermodynamic and kinetic aspects is needed to give a firm conclusion on whether the formation of pyrimidines is more competitive than other side reactions. In this context, we limited ourselves to investigate in the present study several possible mechanistic routes that can lead to pyrimidine bases. We only aim to prove the probability of free radical mechanisms for their formation. The effect of temperature on these suggested mechanisms is also examined to validate their applicability for high-temperature conditions.

2. COMPUTATIONAL DETAILS

The energy profiles associated with the free radical mechanisms were constructed using density functional theory (DFT) method implemented in the Gaussian09 suite of program.[27]

DOI: 10.1021/acs.jpca.5b03625
J. Phys. Chem. A XXXX, XXX, XXX−XXX

Geometries of all the species involved were optimized using the hybrid B3LYP functional[28,29] with the 6-311G(d,p) basis set.[30] The unrestricted formalism (UB3LYP) is used for the open-shell structures. Vibrational frequency analyses were performed at the same level of theory to obtain the zero-point correction energy (ZPE) and to confirm the nature of each stationary point. A uniform scaling factor of 0.967 is used for the ZPE values when calculating the relative energies of the structures considered.

The popular B3LYP functional was employed in several previous studies to explore the production of purine nucleobases in both neutral and free radical states under prebiotic conditions.[5,6,31,32] These studies showed that the difference between B3LYP and CCSD(T) reaction barriers are relatively small, being less than 3 kcal/mol. The performance of the B3LYP/6-311G(d,p) method for radical pathway is revalidated in the present work for a short reaction chain starting from FM **1** to the radical species **6** as plotted in Scheme S1. The CCSD(T) single-point calculations were performed using the B3LYP/6-311G(d,p) optimized geometries of the relevant species. It has been established that the B3LYP functional tends to underestimate the energy barriers for hydrogen addition to multiple bonds[33] or hydrogen abstraction[34] processes. The relevant intermolecular distances in the transition structures are relatively too long as compared to the corresponding CCSD(T) values.[33,34] Therefore, the use of B3LYP optimized geometries for single-point CCSD(T) computations to derive the energy barriers for H addition or abstraction reactions still induces a certain underestimation.

For further tests, two basis sets used for the CCSD(T) calculations include 6-311G(d,p) and aug-cc-pVTZ. The total energies of these species are calculated using the CCSD(T) energies and the B3LYP ZPE corrections. The results are given in Table 1. There was a quite large difference between the CCSD(T) and B3LYP relative energies when the same basis set 6-311G(d,p) was used for both methods. However, using a larger basis set for CCSD(T) computations the differences between two sets of data became smaller, with the largest difference being ±3 kcal/mol.

Table 1. Relative Energies Obtained at the B3LYP/6-311G(d,p), CCSD(T)/6-311G(d,p) and CCSD(T)/aug-cc-pVTZ Levels for Several Species Involved in the Radical Reaction Pathways Leading to Formation of Nucleobases from FM

	relative energies (kcal/mol)		
	B3LYP	CCSD(T)	
	6-311G(d,p)	6-311G(d,p)	aug-cc-pVTZ
1	0	0	0
ts-1,2	2	7	5
2	−18	−14	−16
ts-2,4	7	9	7
4	−18	−17	−19
5	5	3	3
ts-5,6	9	11	9
6	−25	−24	−26

3. RESULTS AND DISCUSSION

3.1. Reaction Initiation and Catalytic Effects of the •CN/HCN and $^{\bullet}NH_2/NH_3$ Pairs. The free radical mechanisms for the synthesis of nucleobases from FM feasible on atmosphere of Titan have emphasized the importance of •CN both as a building unit, similar to FM, and as a reaction initiation for the formation of purine and pyrimidine rings and for the catalytic effects of •CN/HCN and $^{\bullet}NH_2/NH_3$ pairs in the H-rearrangement reactions.[5−8] Because these H-rearrangement reactions make up a significant part of the free radical mechanisms, it is important to determine the most favored condition for them. Obviously, when a species can provide lower barrier and is regenerated somewhere along the reaction paths, it can be considered as a catalyst. The remaining problem is thus to determine the better catalyst pair, •CN/HCN or $^{\bullet}NH_2/NH_3$, for these processes.

Formation of precursor **9** in the previously reported prebiotic mechanism[5,6] is now re-examined to evaluate and compare the catalytic effects of •CN/HCN and $^{\bullet}NH_2/NH_3$ pairs. The step-by-step mechanism and the schematic potential energy profiles leading to **9** are presented in Scheme S1 and Figure S1, respectively, of the Supporting Information. Let us remind that all tables, schemes, and figures labeled first with letter S refer to those given in the Supporting Information.

The one-step 1,3-H radical rearrangements **2** → **4** and **7** → **9** have relatively high energy barriers of 25 and 22 kcal/mol, respectively.[5] With the involvement of $^{\bullet}NH_2/NH_3$ pair, the 1,3-H radical rearrangement becomes a two-step process with the H abstraction by $^{\bullet}NH_2$ (**3-cp** → **4** and **8-cp** → **9**) being the rate-determining step (cf. Figure S1, black bars). This multistep route is much easier to achieve than the one-step one with the energy barriers ($\Delta E^{\#}$) for both transformations **2** → **4** and **7** → **9** now being reduced to 8 kcal/mol.

The •CN/HCN pair can also be used to initiate this multistep 1,3-H rearrangement(cf. Figure S1, green bars). However, this pathway has larger energy barriers for both elementary processes and thus is less favored as compared to the $^{\bullet}NH_2/NH_3$ one. Therefore, the $^{\bullet}NH_2/NH_3$ pair will be used as an initiation and catalyst for the H radical rearrangement.

As for a convention, a transition structure (TS) connecting two equilibrium structures, for example, **A** and **B**, in the $^{\bullet}NH_2/NH_3$ pathways is denoted as **ts-A,B**. The same convention is also applied for all TS's involved in the formation of pyrimidines presented in the following sections. For the •CN/HCN related pathways, the TS's are denoted as **ts-A,B-CN**. The TS's for reactions **2** → **4** and **7** → **9** mentioned above are given in Figure S2.

3.2. Formation of Cytosine. *3.2.1. From Formamide and HCN.* Both the five-membered ring of purines and the six-membered ring of pyrimidines can be formed from the nitrogen-centered radical **9**. The purine ring is simply formed by intramolecular radical attack of •NH group on the C≡N triple bond as previously reported ($\Delta E^{\#}$: 15 kcal/mol).[5] It is obvious from the structure of **9** that an extra carbon atom is needed to complete the chemical frame of pyrimidine ring. This can be done by adding an HCN molecule to **9** via an intermolecular free radical attack on the C≡N bond to form the nitrogen-centered radical **10** as presented in Scheme 2. This pathway is consistent with Yamada's suggestion[35] that cytosine is formed from two FM and two HCN molecules, even not under Titan condition. Note that two FM and one HCN molecules have been consumed to form **9** (cf. Scheme S1). This radical-attack-CN reaction, even though it has the same nature as the purine ring formation from **9**,[5,6] has a much lower energy barrier ($\Delta E^{\#}$: 8 kcal/mol). In both cases, the conversion

DOI: 10.1021/acs.jpca.5b03625
J. Phys. Chem. A XXXX, XXX, XXX−XXX

Scheme 2. Main Route Leading to Formation of Cytosine 22 from Nitrogen-Centered Radical 9

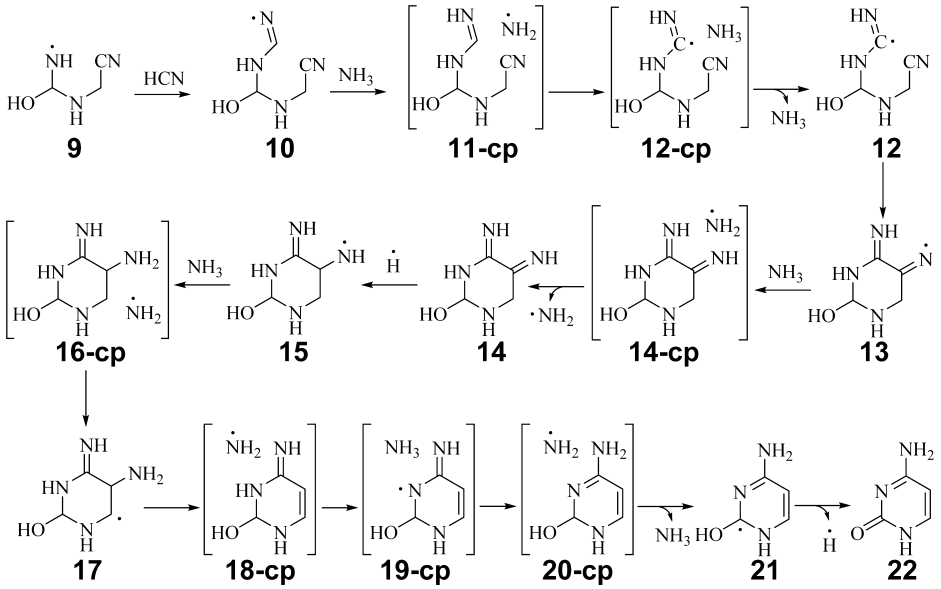

of the CN triple to double bond releases energy and thus makes the reaction exergonic. The energy release of the reaction **9** → **10** is −14 kcal/mol. The potential energy profiles and the participating transition structures of the reaction pathway from the radical intermediate **9** to cytosine (**22**) are plotted in Figures 1 and 2, respectively. The transition structures of several important reaction steps (HCN addition **9** → **10**, cyclization **12** → **13**, and NH_2 loss **17** → **18-cp**) are also indicated in Figure 1. The role of the C≡N as energy reservoir due to the large amount of bond energy released from its partial bond breaking has previously been suggested.[36]

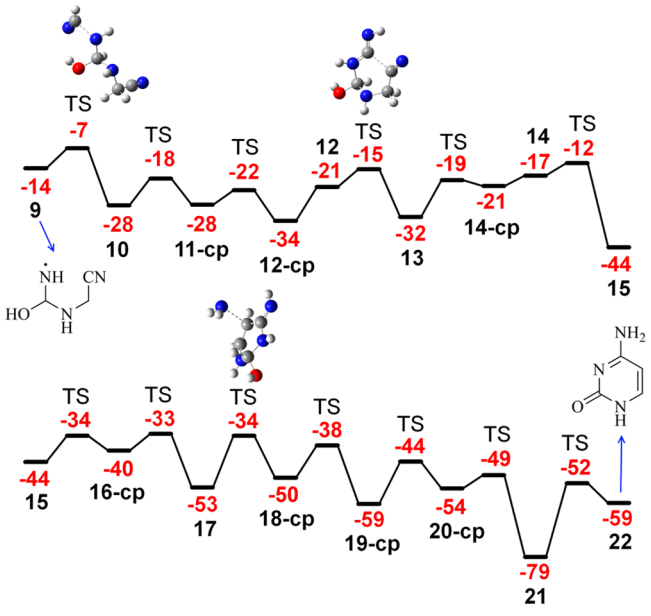

Figure 1. Schematic potential energy profiles for the main route leading to cytosine **22** from nitrogen-centered radical **9**. Relative energies in kcal/mol were obtained from (U)B3LYP/6-311G(d,p) + ZPE computations.

The sp^2 imino carbon-centered radical **12** is formed from **10** via the $^{\bullet}NH_2/NH_3$-assisted 1,2-H rearrangement. This overall H-rearrangement is slightly endothermic by 7 kcal/mol with a relatively low energy barrier of 10 kcal/mol. The next step is the intramolecular radical cyclization of **12** in which the highly reactive sp^2 carbon-centered radical attacks the C≡N bond forming the cyclic species **13**. Again, this reaction is exergonic by an amount of −11 kcal/mol upon a partial breaking of the C≡N bond. In addition, this ring closure step has lower energy barrier ($\Delta E^{\#}$: 7 kcal/mol) than the purine five-membered ring formation.

The next reaction steps from **13** to **17** are a series of H radical additions (**13** → **14**, **14** → **15**) and rearrangements (**15** → **16-cp** → **17**). These steps are necessary for the subsequent removal of the NH_2 group (**17** → **18-cp**). Although the H-addition step **13** → **14** is endergonic by an amount of 16 kcal/mol, the relatively large amount of energy release from the addition of an H atom to **14** and the subsequent H-rearrangement makes the whole reaction chain from **13** to **17** exergonic with a net energy release of −21 kcal/mol. These reactions have relatively low energy barriers ($\Delta E^{\#}$: 5−14 kcal/mol, cf. Figure 1, even though these values are expected to be underestimated). The release of NH_2 radical from **17** forms the $^5C{=}^6C$ double bond of cytosine ring within the complex **18-cp**. This reaction has an energy barrier of 19 kcal/mol. All three pyrimidines use the same numbering system, which is indicated in Scheme 1.

The subsequent H-rearrangement (**18-cp** → **21**) includes three elementary steps: the H-abstraction at ^3N position of **18-cp**, H-addition to the external NH group at ^4C position of **19-cp**, and H-abstraction at ^2C position of **20-cp**. This rearrangement reaction is exergonic by −29 kcal/mol and has a relatively low overall energy barrier of 12 kcal/mol. A final H-loss from **21** forms cytosine **22**. This reaction involves a high overall energy barrier of 28 kcal/mol and is endergonic by 20 kcal/mol. Nevertheless, the main pathway leading to cytosine from FM is still highly exergonic with the net gain in energy of −59 kcal/mol.

Scheme 3 presents an alternative pathway leading to the formation of cytosine starting from FM and HCN, denoted as route **7a**, in which the ^4C atom of cytosine is originated from FM rather than HCN. The potential energy profiles and

DOI: 10.1021/acs.jpca.5b03625
J. Phys. Chem. A XXXX, XXX, XXX−XXX

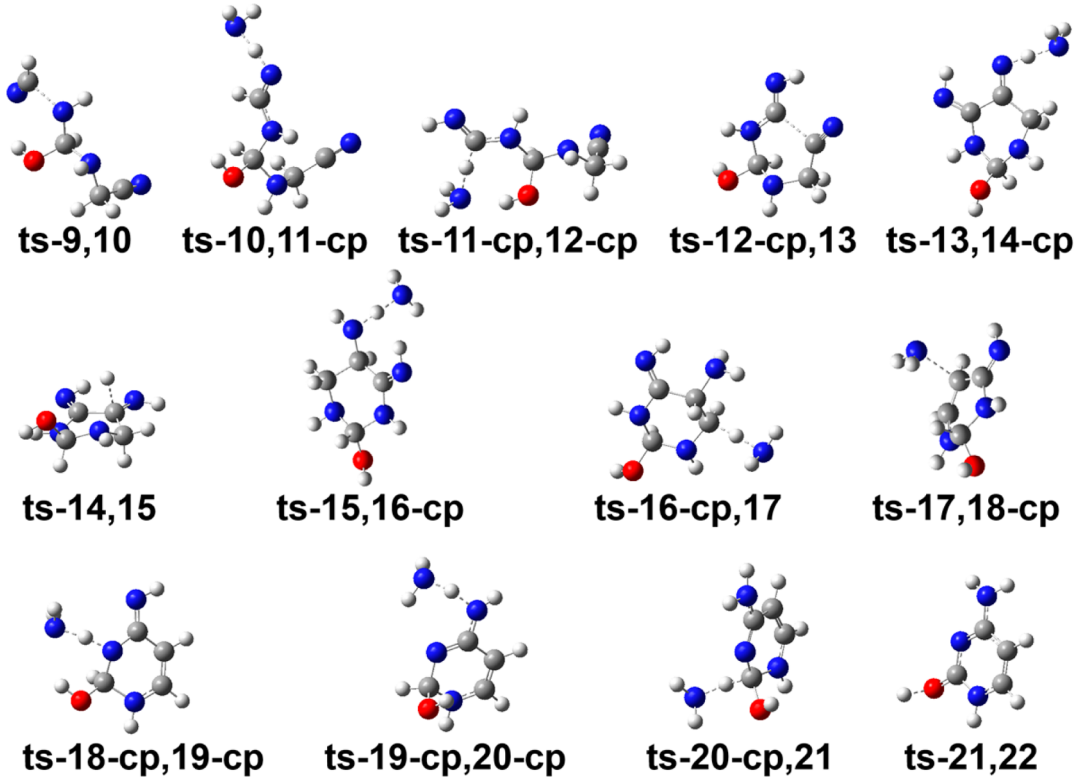

Figure 2. Transition structures involved in the main route leading to cytosine **22** from nitrogen-centered radical **9**.

Scheme 3. Route 7a Leading to Formation of Cytosine 22 from Oxygen-Centered Radical 7

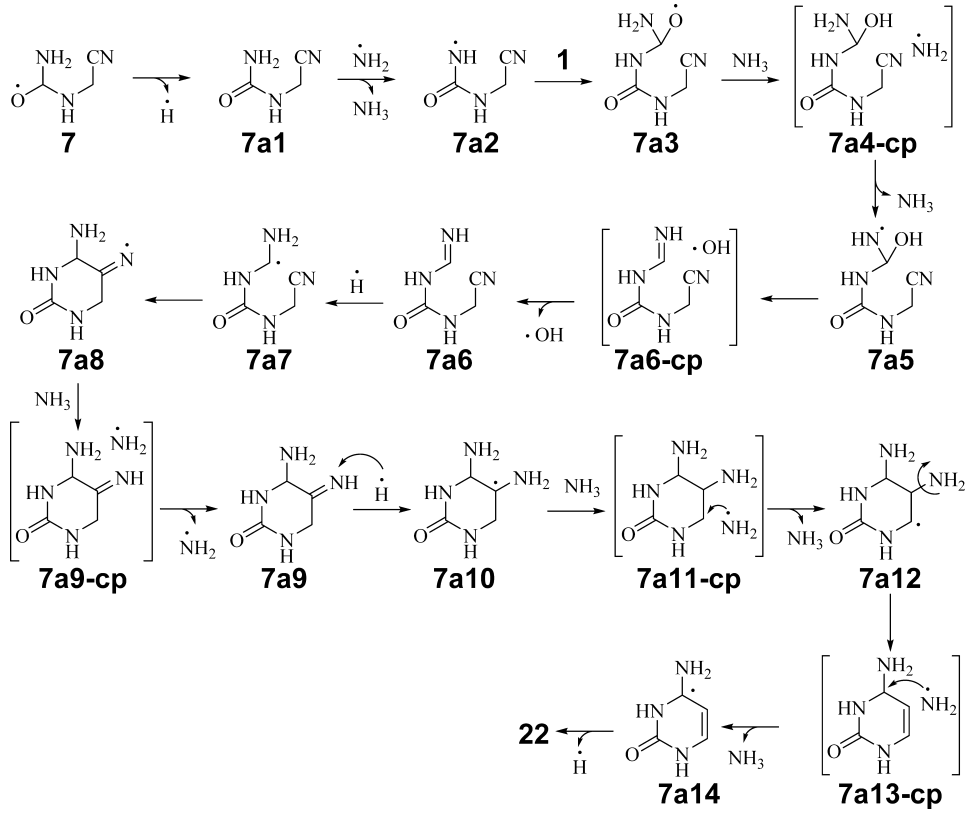

structures of all the relevant TS's for this route are plotted in Figure 3 and Figure S3, respectively. The transition structures of several important reaction steps (FM addition **7a2** → **7a3**, OH loss **7a5** → **7a6-cp**, cyclization **7a7** → **7a8**, and NH_2 loss **7a12** → **7a13-cp**) are indicated in Figure 3. Instead of following the H-rearrangement reaction to form **9**, the oxygen-

DOI: 10.1021/acs.jpca.5b03625
J. Phys. Chem. A XXXX, XXX, XXX−XXX

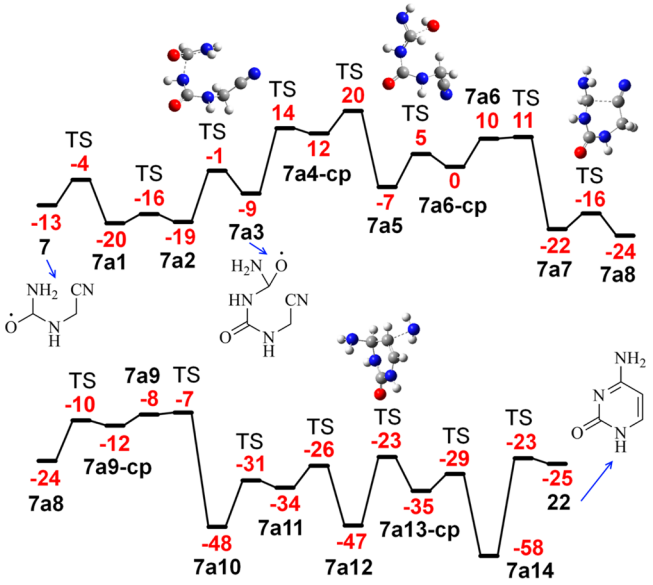

Figure 3. Schematic potential energy profiles for the route **7a** leading to cytosine **22** from oxygen-centered radical **7**. Relative energies in kcal/mol were obtained from (U)B3LYP/6-311G(d,p) + ZPE computations.

centered radical species **7** releases H radical to form the carbonyl group of cytosine in the neutral compound **7a1**. Subsequent H loss from the primary amino group of **7a1** leads to **7a2** with the same NH radical moiety as in the species **9**.

The high diversity of the reaction pathways can clearly be seen at this point. It is easy to note that the addition of HCN to **7a2** can also lead to another alternative pathway for the formation of cytosine. It can be expected that this route is quite similar to the main route because they both use one FM and two HCN molecules to build cytosine. The difference is that the carbonyl group is formed at the beginning instead of at the end of the pathway. The energy of the highest-lying TS in the **7** → **7a2** process is very close to that of the **7** → **9** reactions, with an energy difference of less than 1 kcal/mol. This suggests that both pathways starting from **7** are energetically plausible. A different ordering of the functional group formation gives rise to a large number of possible synthetic routes whose important elementary steps vary slightly from one to another. The alternative pathway via route **7a** leading to a major difference in the chemical constituent of cytosine is thus of more importance to explore.

The NH radical moiety in **7a2** attacks the carbonyl group of FM molecule forming the oxygen-centered radical **7a3**. This radical attack is endergonic by 10 kcal/mol and has higher energy barrier ($\Delta E^{\#}$ = 18 kcal/mol) than the radical attack to the CN triple bond **9** → **10**. With both NH_2 and OH groups (formed from H addition to the O radical) as substituents at ^{4}C position, **7a3** can lead to either cytosine or uracil, depending on the elimination of these two functional groups. Formation of cytosine is achieved by elimination of •OH (**7a5** → **7a6**) preceded by the catalyzed tautomerization/rearrangement (**7a3** → **7a5**). This H-rearrangement has a low energy barrier of 8 kcal/mol. The •OH loss has lower energy barrier of 12 kcal/mol, but the reaction is endergonic by 17 kcal/mol.

The reaction steps of **7a2** → **7a6** can be considered as a free radical analogue of the formiminylation (formylation + dehydration) in the neutral paths forming purine and adenine from FM.[37] The addition of H radical to **7a6** leads to the formation of the sp^3 carbon-centered radical **7a7** with the NH_2 substituent at ^{4}C position. The B3LYP energy barrier of only 1 kcal/mol for this highly exergonic reaction is expected to

Scheme 4. Route 1a Leading to Formation of Cytosine 22 from Formamide and Acetylene

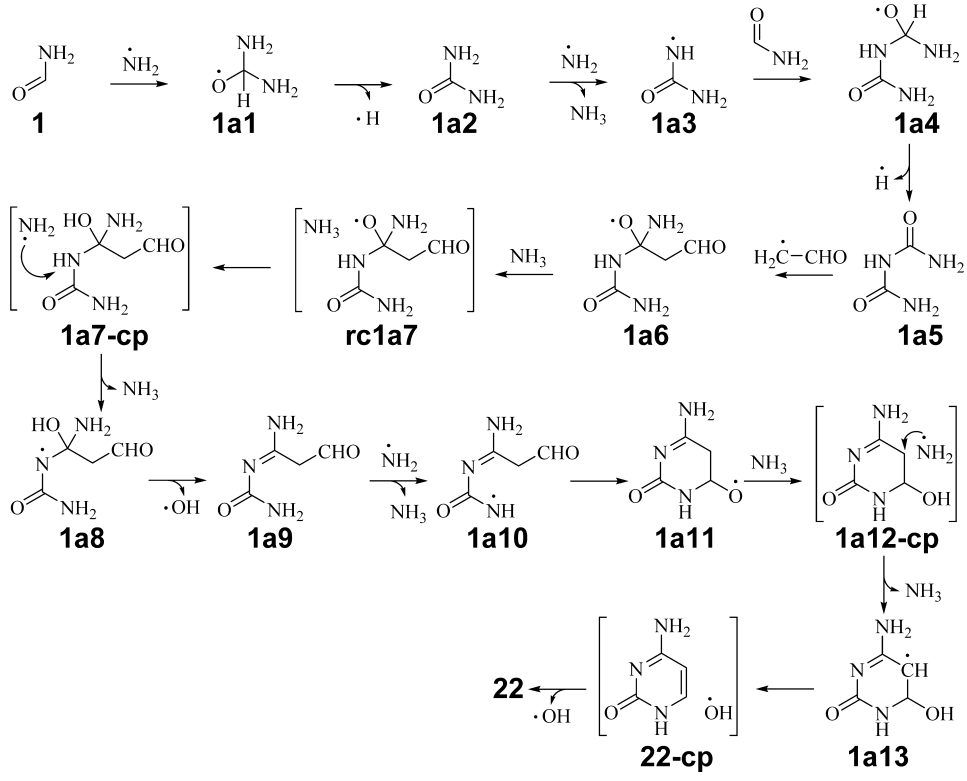

DOI: 10.1021/acs.jpca.5b03625
J. Phys. Chem. A XXXX, XXX, XXX−XXX

significantly be underestimated. Taking such an intrinsic underestimation into account, the corresponding energy barrier remains low.

The following steps of the route **7a** are now similar to that of the main route with the close resemblance between the two potential energy profiles (Figures 1 and 3) such as the low barrier and exergonic intramolecular radical cyclization (**7a7** → **7a8** vs **12** → **13**), highly exergonic H addition (**7a9** → **7a10** vs **14** → **15**), high barrier NH_2 loss (**7a12** → **7a13-cp** vs **17** → **18-cp**), and consecutive H abstraction/removal reactions with the assistance of $^{\bullet}NH_2/NH_3$ pair. Although the relative energy of the ring precursor **7a7** is close to that of the corresponding species **12** in the main pathway, the route **7a** is still much less favored with the highest species **7a6** being 24 kcal/mol higher than 7. Meanwhile, the highest-lying TS in going from 7 to **12** is only 8 kcal/mol higher than 7. With a total gain in energy of 25 kcal/mol in going from FM to cytosine, the alternative route **7a** is both thermodynamically and kinetically less favored than those of the main route.

3.2.2. From Formamide and Acetylene. In the free radical mechanism for formation of pyrimidine bases from FM and acetylene presented in Scheme 4, cytosine is formed from two FM and one acetylene (C_2H_2) molecules. Hydration of acetylene yields acetaldehyde (CH_3CHO), which subsequently releases a H radical to form a carbon-centered radical species $^{\bullet}CH_2CHO$. This acetaldehyde radical prefigures the $^5C{=}^6C$ bond in cytosine (see below). Formation of $^{\bullet}CH_2CHO$ from acetylene is thermodynamically feasible with an energy release of −54 kcal/mol (cf. Figure S4). However, the high energy barrier of 47 kcal/mol of acetylene hydration step makes it kinetically unfavorable.

One FM molecule is transformed into urea (**1a2**) via two steps (**1** → **1a1** → **1a2**), which replace H atom of carbonyl group by NH_2 group. These reactions have an overall energy barrier of 15 kcal/mol as shown in Figure 4. It has been suggested in the urea/acetylene/water experiment that the NH−CO−NH chemical frame of urea makes up the $^1N{-}^2C{-}^3N$ fragment of the pyrimidine bases.[26] The remaining part (^4C) of cytosine can be formed from one-carbon compounds presented in the reaction mixture such as HCN or, as in the route **1a**, the second FM molecule.

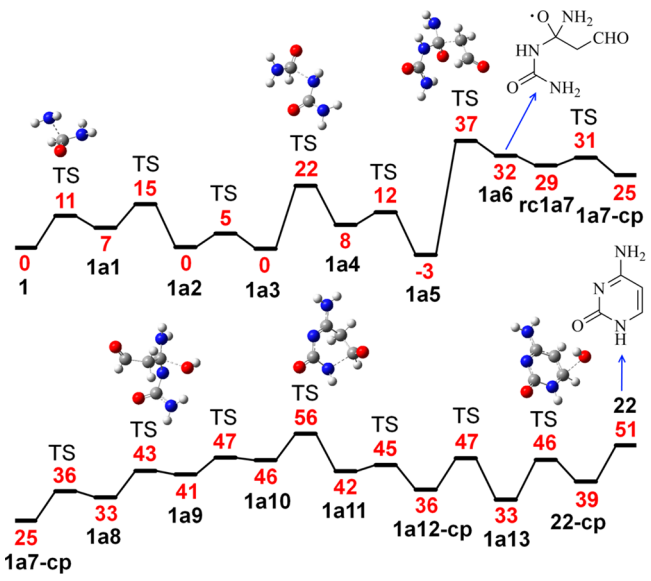

Figure 4. Schematic potential energy profiles for the route **1a** leading to cytosine **22** from FM and acetylene. Relative energies in kcal/mol were obtained from (U)B3LYP/6-311G(d,p) + ZPE computations.

The H radical removal from urea forms nitrogen-centered radical species **1a3**. The $^{\bullet}NH$ radical group of **1a3** attacks the carbonyl group of the second FM molecule with a relatively high energy barrier of 22 kcal/mol. A H loss from **1a4** generates neutral species **1a5** with two equivalent electrophilic carbonyl groups open for a radical addition reaction with the $^{\bullet}CH_2CHO$ species (generated from acetylene as described above). This step completes the chemical frame of the cytosine ring. However, the reactivity of $^{\bullet}CH_2CHO$ appears to be much weaker than that of the nitrogen-centered radical compounds. The **1a5** → **1a6** energy barrier is 40 kcal/mol, being much higher than those of the **6** → 7 (14 kcal/mol), **7a2** → **7a3** (18 kcal/mol), and **1a3** → **1a4** (22 kcal/mol) reactions.

The remaining steps include ring formation and substituent modification. The reaction sequence from **1a6** to **1a9** generates the correct substitution feature at ^3N and ^4C positions. The ring formation step **1a10** → **1a11** is preceded by a H loss in which the nucleophilic NH radical group is formed. Different from previous cases, the intramolecular cyclization step in this route is due to a radical attack to the carbonyl group rather than to the CN. Nevertheless, this reaction still has a low energy barrier of 9 kcal/mol and is slightly exergonic.

The H-rearrangement steps **1a11** → **1a13** are needed for the removal of OH radical that eventually leads to cytosine. Although this route **1a** has fewer steps than the main route presented in Scheme 1, it is thermodynamically and kinetically less favored than the latter. The former is endergonic by 51 kcal/mol, and the highest TS is located at 56 kcal/mol with respect to the reference. All the TS's involved in the route **1a** are plotted in Figure S5.

3.3. Formation of Uracil. *3.3.1. From Formamide and HCN.* Two possible reaction routes are suggested for the synthesis of uracil from FM and HCN, namely, the main route (FM → 7 → **9** → cytosine, uracil, thymine, Scheme 1) and the alternative route **7b**. In the main route presented in Scheme 5, an enol tautomer **24** of uracil is formed from cytosine by replacing the NH_2 substituent by OH group. This substituent replacement takes place via two steps including the addition of OH radical to the ^4C position and the elimination of more stable NH_2 radical. The potential energy profile and the transition structures of this route are plotted in Figures 5 and S6 with the relative energy of cytosine taken from the main route in Scheme 1. Both steps have low energy barriers with the second step being exergonic by 19 kcal/mol. The NH_2 radical in the product complex **24-cp** facilitates the enol−keto tautomerization leading to a slightly more stable keto form **26** of uracil. The complex of uracil and NH_2 radical **26-cp1** is also presented here because it is involved in the formation of thymine (discussed in a following section). Formation of uracil from FM and HCN in this main route is thermodynamically feasible with an overall gain in energy of −81 kcal/mol.

The alternative route **7b** presented in Scheme 6 and Figures 6 and S7 originates from the compound **7a3** in the route **7a**. As previously mentioned, this route allows a simultaneous production of both cytosine and uracil from FM. Instead of a $^{\bullet}OH$ loss from **7a3** to generate the NH_2 substituent, the NH_2 group is now removed in the reaction step **7a3** → **7b1** to form the carbonyl group at the ^4C position. The addition of an H radical to the carbonyl oxygen **7b1** → **7b2** creates a radical at the ^4C center, which subsequently attacks the triple CN bond

DOI: 10.1021/acs.jpca.5b03625
J. Phys. Chem. A XXXX, XXX, XXX−XXX

Scheme 5. Main Route Leading to Formation of Uracil 26 from Cytosine 22

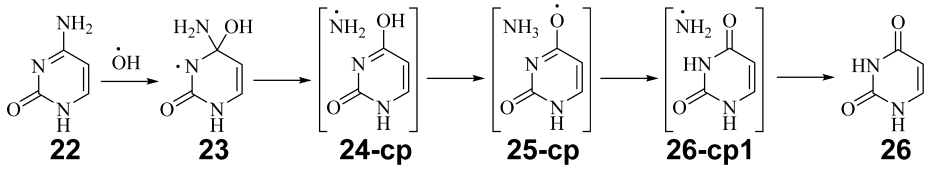

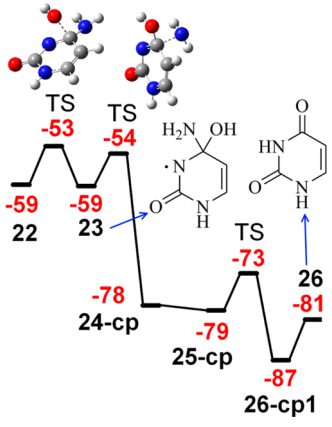

Figure 5. Schematic potential energy profiles for the main route leading to of uracil **26** from cytosine **22**. Relative energies in kcal/mol were obtained from (U)B3LYP/6-311G(d,p) + ZPE computations.

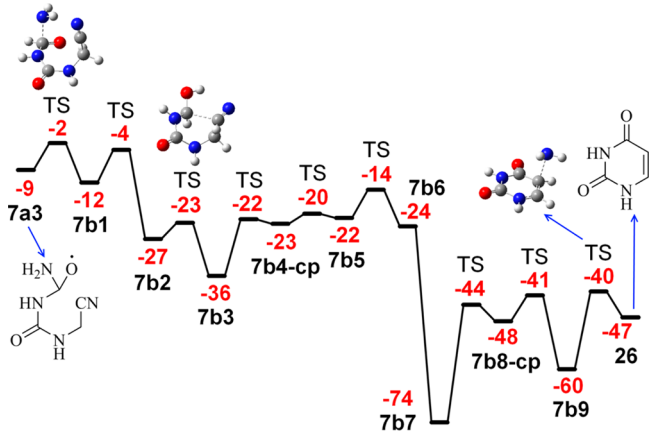

Figure 6. Schematic potential energy profiles for the route **7b** leading to uracil **26** from oxygen-centered radical **7a3**. Relative energies in kcal/mol were obtained from (U)B3LYP/6-311G(d,p) + ZPE computations.

in the ring-closing step **7b2** → **7b3**. The recovery of a carbonyl group and the removal of the substituent at ^{5}C position are achieved via a series of H-abstraction/addition reactions. An overall gain in energy of −47 kcal/mol is obtained when uracil is formed via the route **7b**, whereas that of cytosine formation via route **7a** brings in only −25 kcal/mol. Such a difference of 22 kcal/mol between formation of cytosine and uracil, with the latter being more favored, is the same as that of the main route. In addition, uracil generation via route **7b** also has a lower overall energy barrier than that of cytosine formation via route **7a**. The system does not require additional energy to cross the highest transition structure **ts-7a2,7a3** in the former pathway, whereas an extra energy of 20 kcal/mol is required in the latter case.

3.3.2. From Formamide and Acetylene. The route **1b** (cf. Scheme 7 and Figures 7 and S8) is a branch of the route **1a** with the branching position **1a6**, similar to **7a3**, having two functional groups at the ^{4}C position. The carbonyl group at ^{4}C position of uracil is thus formed from the NH_2 loss **1a6** → **1b1-cp** whose energy barrier is, however, 7 kcal/mol higher than that of the **7a3** → **7b1**. Similar to the route **1a**, the ring-closing step **1b2** → **1b3** in this route is due to the attack of NH radical moiety to the carbonyl group with the very low energy barrier of 3 kcal/mol. Obviously, the intramolecular radical cyclization is an efficient way to form a ring in prebiotic synthesis.

The six-membered ring **1b3** can either follow a H loss to generate the neutral barbituric acid (**BA**) or continue a series of H-exchange reactions before detaching the OH radical group finally giving uracil. Although the H-exchange series is slightly thermodynamically favored, the OH loss is endergonic by 22 kcal/mol. This makes uracil production via route **1b** endergonic by 30 kcal/mol. Similar to the route **1a**, a large amount of additional energy of 46 kcal/mol is needed to overcome the highest energy barrier of the route **1b** and thereby renders it kinetically unfavorable.

3.4. Formation of Thymine. Thymine can be formed from uracil by replacing the H atom at the ^{5}C position by a CH_3

Scheme 6. Route 7b Leading to Formation of Uracil 26 from Oxygen-Centered Radical 7a3

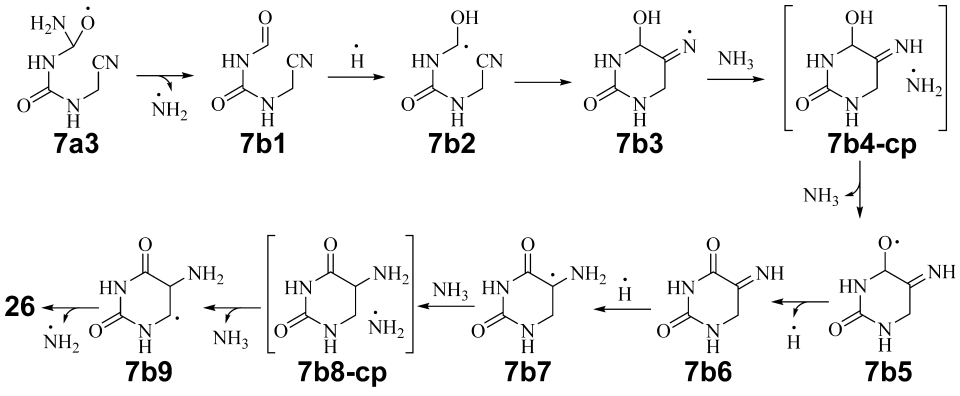

DOI: 10.1021/acs.jpca.5b03625
J. Phys. Chem. A XXXX, XXX, XXX−XXX

Scheme 7. Route 1b Leading to Formation of Uracil 26 and Barbituric Acid (BA) from Oxygen-Centered Radical 1a6

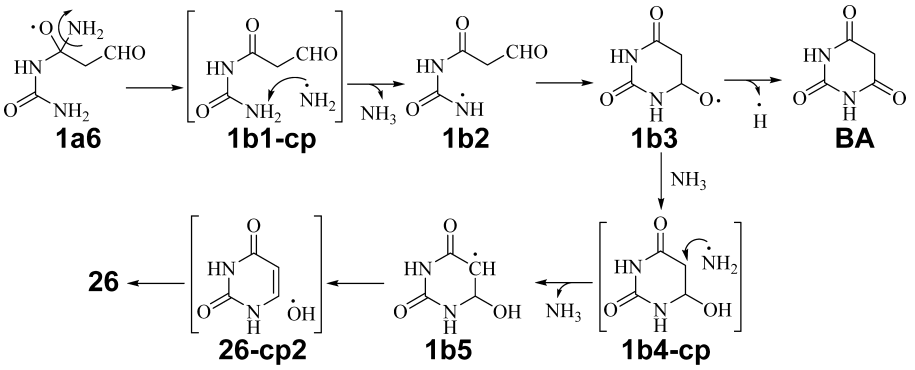

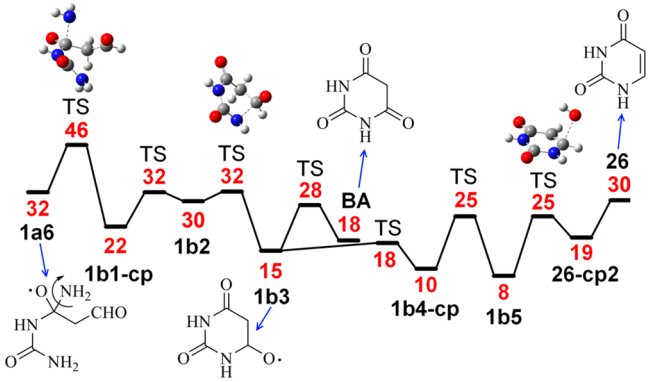

Figure 7. Schematic potential energy profiles for the route **1b** leading to uracil **26** and barbituric acid BA from oxygen-centered radical **1a6**. Relative energies in kcal/mol were obtained from (U)B3LYP/6-311G(d,p) + ZPE computations.

group. This methyl substituent can be added using one-carbon compounds available in the reaction mixture. The reaction of uracil and methylene in the gas phase was studied theoretically using computations at CCSD(T)//B3LYP level.[38] The results show that methylene preferentially attacks the ^{1}N position of uracil forming 1-methyluracil instead of thymine. The presence of 5-hydroxymethyluracil, N9-formylpurine, and N6,N9-diformyladenine in the product mixture after heating and irradiating FM with TiO_2 as catalyst suggests the involvement of $H_2C{=}O$ in thymine formation.[16] The theoretical investigation of this acetaldehyde-involved mechanism under free radical condition has, however, not been explored yet. In the present paper, two free radical mechanisms for the formation of thymine from uracil and formaldehyde are examined. The difference between both mechanisms lies in the transformation of the alcohol group formed from the addition of formaldehyde to the ^{5}C position of uracil to form the methyl substituent of thymine.

In the main mechanism yielding thymine from the uracil complex **26-cp1** presented in Scheme 8 and Figures 8 and S9,

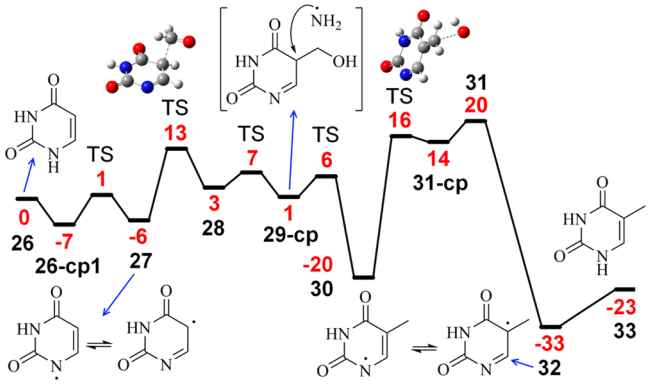

Figure 8. Schematic potential energy profiles for the main route leading to thymine **33** from uracil **26**. Relative energies in kcal/mol were obtained from (U)B3LYP/6-311G(d,p) + ZPE computations.

H loss at ^{1}N position of uracil generates the nitrogen-centered radical **27**. The conjugated form of **27** with the radical center located at the ^{5}C atom (sp^3) can subsequently react with $H_2C{=}O$ yielding the oxygen-centered radical of 5-hydroxymethyluracil **28**. The next H-rearrangement step **28** → **29-cp** → **30** gives the carbon-centered radical of 5-hydroxymethyluracil **30**, which is much more stable than the oxygen-centered

Scheme 8. Main Route Leading to Formation of Thymine 33 from Uracil 26

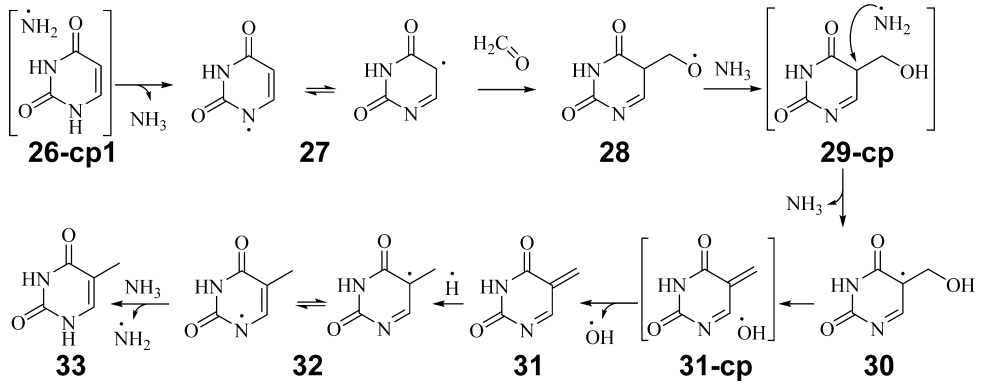

DOI: 10.1021/acs.jpca.5b03625
J. Phys. Chem. A XXXX, XXX, XXX−XXX

Scheme 9. Route 26a Leading to Formation of Thymine 33 from Uracil 26

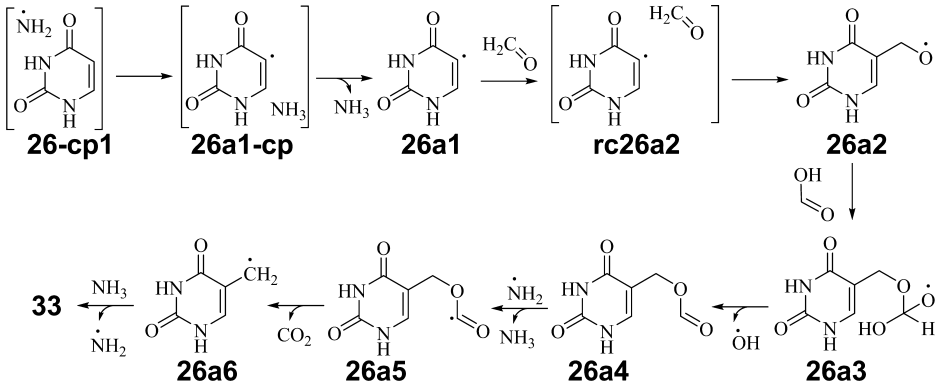

radical **28**. The following OH loss **30** → **31** is, however, highly endergonic with an absorbed energy of 40 kcal/mol. The two-step radical hydrogenation turns the methylene group in the neutral product **31** into the methyl group of thymine **33**. The large amount of energy released from the first H-addition step **31** → **32** compensates the energy taken in the previous steps and thus makes this whole reaction chain exergonic by −23 kcal/mol.

The NH_2 radical of **26-cp1** can also attack the uracil ring at the ^5C instead of ^1N position to form the sp^2 carbon-centered radical **26a1**, which is 15 kcal/mol less stable than its sp^3 carbon-centered radical isomer **27**(cf. Scheme 9 and Figures 9

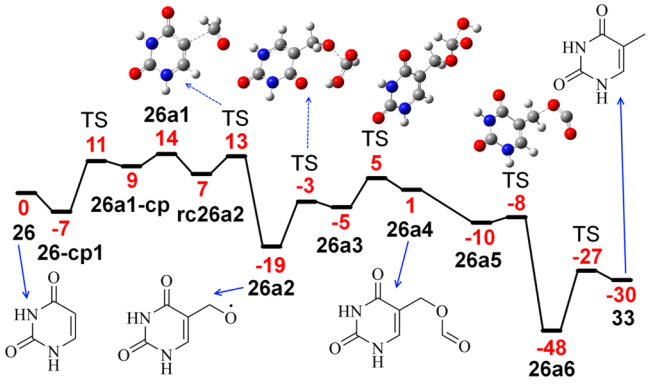

Figure 9. Schematic potential energy profile for the route **26a** leading to thymine **33** from uracil **26**. Relative energies in kcal/mol were obtained from (U)B3LYP/6-311G(d,p) + ZPE computations.

and S10). The former is however more reactive with an energy barrier for the reaction between **26a1** and acetaldehyde, being 12 kcal/mol lower than that of the corresponding **27** → **28** reaction. The oxygen-centered radical product **26a2** of this reaction is also more stable than its isomer **28**. Emergence of CH_3 group in thymine from **26a2** follows a completely different route as compared to the main pathway mentioned above. The oxygen-centered radical **26a2** reacts with formic acid to form an ester compound **26a4** via two endergonic steps. The H abstraction at carbon atom of acid fragment yields the sp^2 carbon-centered radical **26a5**, which releases CO_2 to form more stable sp^3 carbon-centered radical **26a6**. The deoxygenation reduction of the alcohol group in 5-hydroxymethyluracil via the addition of formic acid and decarbonylation has been previously suggested.[3,16,39] Although the ester-forming step **26a2** → **26a4** is endergonic by 20 kcal/mol, the next two steps, which remove the stable CO_2 molecule, are highly exergonic with the release energy of −50 kcal/mol in going from **26a4** to **26a6**. The final endergonic H-addition step yields thymine with the energy barrier of 21 kcal/mol. Compared to the main route, the route **26a** converting uracil to thymine has a lower overall barrier (14 kcal/mol) and releases a larger amount of energy (−30 kcal/mol). However, the fact that the sp^2 carbon-centered radical **26a1** is less stable than the sp^3 carbon-centered radical **27** can affect the feasibility of the route **26a**.

3.5. Effect of Temperature on the Free Radical Mechanisms. The enthalpy barriers, enthalpies of reactions, Gibbs free energy barriers, and Gibbs free energies of reactions at 94 K (being the surface temperature of Titan[40]), 298 K (the commonly used standard ambient temperature), and 483 K (being the boiling point of formamide) were calculated to investigate the effect of temperature on the suggested mechanisms. Energy, enthalpy, and Gibbs free energy profiles of the main routes are plotted in Figure 10 in black, blue, and

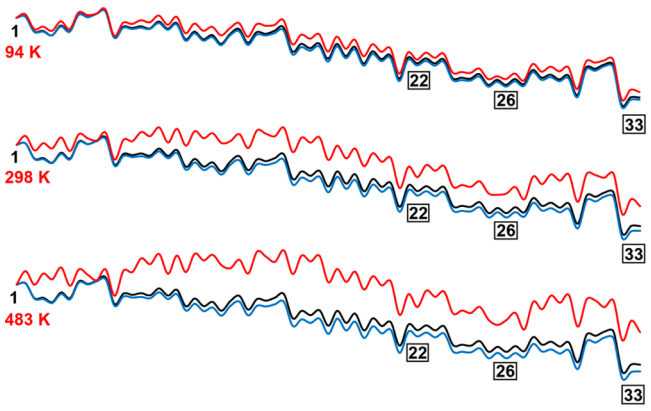

Figure 10. Energy, enthalpy, and Gibbs free energy profiles (black, blue, and red, respectively) of the main routes leading to the formation of cytosine **22**, uracil **26**, and thymine **33** from FM at 94, 298, and 483 K. Relative energies, given in kcal/mol, were obtained from (U)B3LYP/6-311G(d,p) + ZPE computations.

red, respectively. The three profiles are close together at low temperature, but the differences increase at higher temperatures. As clearly pointed out in Figure 10, the variation with respect to temperature of the Gibbs free energy profiles is much more profound than that of the enthalpy profiles. The overall energy, enthalpy, Gibbs free energy barriers ($\Delta E^{\#}$, $\Delta H^{\#}$, and $\Delta G^{\#}$), the overall reaction energies (ΔE_R), enthalpies of reactions (ΔH_R), and Gibbs free energies of reactions (ΔG_R) for the main routes are given in Table 2. The data show

DOI: 10.1021/acs.jpca.5b03625
J. Phys. Chem. A XXXX, XXX, XXX−XXX

Table 2. Overall Energy Barriers and Reaction Energies ($\Delta E^{\#}$, ΔE_R), Enthalpy Barriers, Enthalpies of Reaction ($\Delta H^{\#}$, ΔH_R), Gibbs Free Energy Barriers, and Gibbs Free Energies of Reaction ($\Delta G^{\#}$, ΔG_R) in kcal/mol at Different Temperatures of the Main Routes Leading to the Formation of Cytosine 22, Uracil 26, and Thymine 33 from Formamide

		94 K		298 K		483 K	
	$\Delta E^{\#}$	$\Delta H^{\#}$	$\Delta G^{\#}$	$\Delta H^{\#}$	$\Delta G^{\#}$	$\Delta H^{\#}$	$\Delta G^{\#}$
1 →**22**	9	9	11	8	22	7	44
1 →**26**							
1 →**33**							
	ΔE_R	ΔH_R	ΔG_R	ΔH_R	ΔG_R	ΔH_R	ΔG_R
1 →**22**	−59	−62	−54	−65	−41	−67	−29
1 →**26**	−81	−83	−76	−86	−64	−89	−52
1 →**33**	−104	−107	−97	−110	−78	−113	−62

obviously unfavorable changes of the overall $\Delta G^{\#}$ and ΔG_R upon increasing temperature. The overall barrier $\Delta G^{\#}$ steadily increase from 11 kcal/mol at 94 K to 22 and 44 kcal/mol at 298 and 483 K, respectively. Although the reaction mechanisms become less exergonic as the temperature increases, the overall ΔG_R values for the formation of cytosine, uracil, and thymine at 483 K remain highly negative, being −29, −52, and −62 kcal/mol, respectively. Our calculations show that the sign of the overall ΔG_R changes from negative to positive at the temperatures of ∼900, 1300, and 1200 K for the formation of cytosine, uracil, and thymine, respectively. At these temperatures, the overall $\Delta G^{\#}$ increase to much larger values of 102, 163, and 148 kcal/mol, respectively.

The enthalpy and Gibbs free energy data for the alternative routes are tabulated in Table S3. The same unfavorable changes are observed for the overall $\Delta G^{\#}$ and ΔG_R of the reaction pathways leading to the formation of pyrimidines from FM and acetylene, routes **1a** and **1b**. However, increasing temperature conversely affects the overall $\Delta G^{\#}$ and ΔG_R of the alternative routes **7a**, **7b**, and **26a**. While the overall $\Delta G^{\#}$ of these pathways behave similarly to the main route and the routes **1a** and **1b**, the overall ΔG_R change favorably as the temperature increases. In general, the main routes are still more favored than the alternative routes, even at the high temperature conditions up to 483 K (cf. Table S3).

3.6. Feasibility of the Pathways for the Formation of Pyrimidine Bases and Purines. Free radical pathways are not selective; therefore, the pathways are competitive with alternative routes. In the current study, alternative routes leading to the pyrimidine bases were evaluated. As mentioned above, previous experimental studies suggested that competitive routes lead to the formation of purines together with the pyrimidine bases.[7,12−22] We recently reported alternative pathways leading to purine nucleobases (hypoxanthine, adenine, purine, guanine, isoguanine, xanthine)[5,6] from FM (Scheme 1). These pathways are expected to compete with formation of the pyrimidine bases. There are major similarities in the types of reactions leading to both pyrimidine and purine bases. For example, some steps involved in the formation of both pyrimidine bases and purines include: hydrogen abstractions, hydrogen rearrangements, and cyclization steps. Also, these types of reactions can take place with intermediates and may lead to byproducts. These side reactions tend to decrease the overall yield. Indeed, these products have been identified experimentally with low yields.[16,18] A novelty of the current study is that the intermediate **9** shown in Scheme 1 unifies the mechanisms for formation of all canonical nucleobases. The potential energy profiles for cytosine, uracil, adenine, and guanine formation correspond to those of both thermodynamically and kinetically achievable processes.

4. CONCLUSIONS

The step-by-step free radical mechanisms giving pyrimidine bases from formamide were investigated in the present work using DFT computations. Several working mechanisms were suggested for the formation of cytosine and uracil in cold conditions, which could apply to prebiotic syntheses in the early Earth. Pyrimidines can be formed from the reactions of FM and HCN or acetylene, the main product of discharging the Titan CH_4/N_2 atmosphere, in the presence of other decomposition products of FM such as $^{\bullet}CN$, $^{\bullet}NH_2$, and NH_3. All of the suggested mechanisms in the present work employed simple radical reactions such as H rearrangement, $^{\bullet}H/^{\bullet}OH/^{\bullet}NH_2$ radical losses, and most importantly intramolecular radical cyclization. The advantages of free radical mechanisms are the inherently low energy barriers, which are observed in most reaction steps and the highly exergonic nature of the whole reaction chain. Because of the rather limited number of reaction pathways being explored, a final conclusion about the most probable pathways leading to pyrimidine bases remains uncertain. However, it is now possible to compare the different suggested pathways for the formation of cytosine (main route, routes **7a** and **1a**), uracil (main route, routes **7b** and **1b**), and thymine (main route and route **26a**). The results suggest that the main routes (FM → **7** → **9** → cytosine, uracil, thymine) are in general more favored than alternative routes. The energy release following formation of cytosine, uracil, and thymine from FM via the main routes amounts to −59, −81, and −104 kcal/mol, respectively. In general, increasing temperature induces unfavorable changes in both kinetic and thermodynamic aspects of the suggested routes. However, the main routes are still more favored than the alternative pathways at the temperature up to the boiling point of FM. Note that these suggested routes are only a few of numerous possible reaction pathways taking place in the reaction mixture. The global potential energy surfaces including all side reactions are thus needed to give a firm conclusion about the results of an actual synthesis.

■ ASSOCIATED CONTENT

Supporting Information

The Supporting Information is available free of charge on the ACS Publications website at DOI: 10.1021/acs.jpca.5b03625.

Reaction barriers and reaction energies in kcal/mol of each reaction step, enthalpy and Gibbs free energy barriers, enthalpies of reactions and Gibbs free energies of reactions of the alternative reaction chains, schematic potential energy profile for the formation of **9** from FM, and transition structures involved in the free radical pathways considered in this work. (PDF)

■ AUTHOR INFORMATION

Corresponding Authors

*E-mail: minh.nguyen@chem.kuleuven.be. (M.T.N.)
*E-mail: yjeilani@spelman.edu. (Y.A.J.)

DOI: 10.1021/acs.jpca.5b03625
J. Phys. Chem. A XXXX, XXX, XXX−XXX

Author Contributions

The manuscript was written with contributions of all authors. All authors have given approval to the final version of the manuscript.

Notes

The authors declare no competing financial interest.

■ ACKNOWLEDGMENTS

We are indebted to the KU Leuven Research Council (GOA and IDO programs) for continuing support. H.T.N. received a KU Leuven doctoral scholarship from an interdisciplinary research project (IDO-2011) on Exoplanets. Y.A.J. acknowledges support from the Research Initiative for Scientific Enhancement (RISE) program. H.M.H. thanks the Vietnam Ministry for Education and Training (Scholarship Program 911).

■ REFERENCES

(1) Oró, J.; Kimball, A. P. Synthesis of Purines under Possible Primitive Earth Conditions. I. Adenine from Hydrogen Cyanide. *Arch. Biochem. Biophys.* **1961**, *94*, 217−227.

(2) Gupta, V. P.; Rawat, P.; Singh, R. N.; Tandon, P. Formation of 2-Imino-malononitrile and Diaminomaleonitrile in Nitrile Rich Environments: A Quantum Chemical Study. *Comput. Theor. Chem.* **2012**, *983*, 7−15.

(3) Schwartz, A. W.; Chittenden, G. J. F. Synthesis of Uracil and Thymine under Simulated Prebiotic Conditions. *BioSystems* **1977**, *9*, 87−92.

(4) Wang, J.; Gu, J. D.; Nguyen, M. T.; Springsteen, G.; Leszczynski, J. From Formamide to Adenine: A Self-Catalytic Mechanism for an Abiotic Approach. *J. Phys. Chem. B* **2013**, *117*, 14039−14045.

(5) Jeilani, Y. A.; Nguyen, H. T.; Newallo, D.; Dimandja, J. M. D.; Nguyen, M. T. Free Radical Routes for Prebiotic Formation of DNA Nucleobases from Formamide. *Phys. Chem. Chem. Phys.* **2013**, *15*, 21084−21093.

(6) Jeilani, Y. A.; Nguyen, H. T.; Cardelino, B. H.; Nguyen, M. T. Free Radical Pathways for the Prebiotic Formation of Xanthine and Isoguanine from Formamide. *Chem. Phys. Lett.* **2014**, *598*, 58−64.

(7) Ferus, M.; Michalcikova, R.; Shestivska, V.; Sponer, J.; Sponer, J. E.; Civis, S. High-Energy Chemistry of Formamide: A Simpler Way for Nucleobase Formation. *J. Phys. Chem. A* **2014**, *118*, 719−736.

(8) Ferus, M.; Nesvorný, D.; Šponer, J.; Kubelík, P.; Michalčíková, R.; Shestivská, V.; Šponer, J. E.; Civiš, S. High-energy Chemistry of Formamide: A Unified Mechanism of Nucleobase Formation. *Proc. Natl. Acad. Sci. U. S. A.* **2015**, *112*, 657−662.

(9) Yamada, H.; Okamoto, T. One-Step Synthesis of Purine Ring from Formamide. *Chem. Pharm. Bull.* **1972**, *20*, 623−624.

(10) Barks, H. L.; Buckley, R.; Grieves, G. A.; Di Mauro, E.; Hud, N. V.; Orlando, T. M. Guanine, Adenine, and Hypoxanthine Production in UV-Irradiated Formamide Solutions: Relaxation of the Requirements for Prebiotic Purine Nucleobase Formation. *ChemBioChem* **2010**, *11*, 1240−1243.

(11) Saladino, R.; Brucato, J. R.; De Sio, A.; Botta, G.; Pace, E.; Gambicorti, L. Photochemical Synthesis of Citric Acid Cycle Intermediates Based on Titanium Dioxide. *Astrobiology* **2011**, *11*, 815−824.

(12) Saladino, R.; Crestini, C.; Costanzo, G.; Negri, R.; Di Mauro, E. A Possible Prebiotic Synthesis of Purine, Adenine, Cytosine, and 4(3H)-Pyrimidinone from Formamide: Implications for the Origin of Life. *Bioorg. Med. Chem.* **2001**, *9*, 1249−1253.

(13) Saladino, R.; Crestini, C.; Neri, V.; Ciciriello, F.; Costanzo, G.; Di Mauro, E. Origin of Informational Polymers: The Concurrent Roles of Formamide and Phosphates. *ChemBioChem* **2006**, *7*, 1707−1714.

(14) Saladino, R.; Barontini, M.; Cossetti, C.; Di Mauro, E.; Crestini, C. The Effects of Borate Minerals on the Synthesis of Nucleic Acid Bases, Amino Acids and Biogenic Carboxylic Acids from Formamide. *Origins Life Evol. Biospheres* **2011**, *41*, 317−330.

(15) Saladino, R.; Crestini, C.; Ciambecchini, U.; Ciciriello, F.; Costanzo, G.; Di Mauro, E. Synthesis and Degradation of Nucleobases and Nucleic Acids by Formamide in the Presence of Montmorillonites. *ChemBioChem* **2004**, *5*, 1558−1566.

(16) Saladino, R.; Ciambecchini, U.; Crestini, C.; Costanzo, G.; Negri, R.; Di Mauro, E. One-Pot TiO_2-Catalyzed Synthesis of Nucleic Bases and Acyclonucleosides from Formamide: Implications for the Origin of Life. *ChemBioChem* **2003**, *4*, 514−521.

(17) Saladino, R.; Neri, V.; Crestini, C.; Costanzo, G.; Graciotti, M.; Di Mauro, E. Synthesis and Degradation of Nucleic Acid Components by Formamide and Iron Sulfur Minerals. *J. Am. Chem. Soc.* **2008**, *130*, 15512−15518.

(18) Shanker, U.; Bhushan, B.; Bhattacharjee, G.; Kamaluddin. Kamaluddin Formation of Nucleobases from Formamide in the Presence of Iron Oxides: Implication in Chemical Evolution and Origin of Life. *Astrobiology* **2011**, *11*, 225−233.

(19) Saladino, R.; Neri, V.; Crestini, C.; Costanzo, G.; Graciotti, M.; Di Mauro, E. The Role of the Formamide/Zirconia System in the Synthesis of Nucleobases and Biogenic Carboxylic Acid Derivatives. *J. Mol. Evol.* **2010**, *71*, 100−110.

(20) Kumar, A.; Sharma, R.; Kamaluddin. Kamaluddin Formamide-Based Synthesis of Nucleobases by Metal(II) Octacyanomolybdate-(IV): Implication in Prebiotic Chemistry. *Astrobiology* **2014**, *14*, 769−779.

(21) Saladino, R.; Crestini, C.; Cossetti, C.; Di Mauro, E.; Deamer, D. Catalytic Effects of Murchison Material: Prebiotic Synthesis and Degradation of RNA Precursors. *Origins Life Evol. Biospheres* **2011**, *41*, 437−451.

(22) Saladino, R.; Botta, G.; Delfino, M.; Di Mauro, E. Meteorites as Catalysts for Prebiotic Chemistry. *Chem. - Eur. J.* **2013**, *19*, 16916−16922.

(23) Saladino, R.; Crestini, C.; Neri, V.; Brucato, J. R.; Colangeli, L.; Ciciriello, F.; Di Mauro, E.; Costanzo, G. Synthesis and Degradation of Nucleic Acid Components by Formamide and Cosmic Dust Analogues. *ChemBioChem* **2005**, *6*, 1368−1374.

(24) Orgel, L. E. Prebiotic Adenine Revisited: Eutectics and Photochemistry. *Origins Life Evol. Biospheres* **2004**, *34*, 361−369.

(25) Nuevo, M.; Milam, S. N.; Sandford, S. A. Nucleobases and Prebiotic Molecules in Organic Residues Produced from the Ultraviolet Photo-Irradiation of Pyrimidine in NH_3 and H_2O+NH_3 Ices. *Astrobiology* **2012**, *12*, 295−314.

(26) Menor-Salván, C.; Marín-Yaseli, M. R. A New Route for the Prebiotic Synthesis of Nucleobases and Hydantoins in Water/Ice Solutions Involving the Photochemistry of Acetylene. *Chem. - Eur. J.* **2013**, *19*, 6488−6497.

(27) Frisch, M. J.; Trucks, G. W.; Schlegel, H. B.; Scuseria, G. E.; Robb, M. A.; Cheeseman, J. R.; Scalmani, G.; Barone, V.; Mennucci, B.; Petersson, G. A. et al. *Gaussian 09,* Revision A.02; Gaussian, Inc.: Wallingford, CT, 2009.

(28) Becke, A. D. Density-Functional Exchange-Energy Approximation with Correct Asymptotic-Behavior. *Phys. Rev. A: At., Mol., Opt. Phys.* **1988**, *38*, 3098−3100.

(29) Lee, C. T.; Yang, W. T.; Parr, R. G. Development of the Colle-Salvetti Correlation-Energy Formula into a Functional of the Electron-Density. *Phys. Rev. B: Condens. Matter Mater. Phys.* **1988**, *37*, 785−789.

(30) Hehre, W. J.; Radom, L.; Schleyer, P. V. R.; Pople, J. A. *Ab Initio Molecular Orbital Theory;* Wiley: Hoboken, NJ, 1986.

(31) Roy, D.; Najafian, K.; Schleyer, P. V. Chemical Evolution: The Mechanism of the Formation of Adenine under Prebiotic Conditions. *Proc. Natl. Acad. Sci. U. S. A.* **2007**, *104*, 17272−17277.

(32) Wang, J.; Gu, J. D.; Nguyen, M. T.; Springsteen, G.; Leszczynski, J. From Formamide to Purine: An Energetically Viable Mechanistic Reaction Pathway. *J. Phys. Chem. B* **2013**, *117*, 2314−2320.

(33) Nguyen, M. T.; Creve, S.; Vanquickenborne, L. G. Difficulties of Density Functional Theory in Investigating Addition Reactions of the Hydrogen Atom. *J. Phys. Chem.* **1996**, *100*, 18422−18425.

DOI: 10.1021/acs.jpca.5b03625
J. Phys. Chem. A XXXX, XXX, XXX−XXX

(34) Nguyen, H. M. T.; Chandra, A. K.; Carl, S. A.; Nguyen, M. T. Quantum Chemical Study of Hydrogen Abstraction Reactions of the Ethynyl Radical with Hydrogen Compounds (C_2H + HX). *J. Mol. Struct.: THEOCHEM* **2005**, *732*, 219−224.
(35) Yamada, H.; Hirobe, M.; Higashiyama, K.; Takahashi, H.; Suzuki, K. T. Reaction Mechanism for Purine Ring Formation as Studied by 13C-15N Coupling. *Tetrahedron Lett.* **1978**, *19*, 4039−4042.
(36) Ferus, M.; Civis, S.; Mladek, A.; Sponer, J.; Juha, L.; Sponer, J. E. On the Road from Formamide Ices to Nucleobases: IR-Spectroscopic Observation of a Direct Reaction between Cyano Radicals and Formamide in a High-Energy Impact Event. *J. Am. Chem. Soc.* **2012**, *134*, 20788−20796.
(37) Hudson, J. S.; Eberle, J. F.; Vachhani, R. H.; Rogers, L. C.; Wade, J. H.; Krishnamurthy, R.; Springsteen, G. A Unified Mechanism for Abiotic Adenine and Purine Synthesis in Formamide. *Angew. Chem., Int. Ed.* **2012**, *51*, 5134−5137.
(38) Wang, T. F.; Bowie, J. H. Can Cytosine, Thymine and Uracil be Formed in Interstellar Regions? A Theoretical Study. *Org. Biomol. Chem.* **2012**, *10*, 652−662.
(39) Choughuley, A. S. U.; Subbaraman, A. S.; Kazi, Z. A.; Chadha, M. S. Possible Prebiotic Synthesis of Thymine - Uracil-Formaldehyde-Formic Acid Reaction. *BioSystems* **1977**, *9*, 73−80.
(40) Mitri, G.; Showman, A. P.; Lunine, J. I.; Lorenz, R. D. Hydrocarbon Lakes on Titan. *Icarus* **2007**, *186*, 385−394.

DOI: 10.1021/acs.jpca.5b03625
J. Phys. Chem. A XXXX, XXX, XXX−XXX